



Ab initio calculations of the effect of N, Nb, and Ta doping on the electronic structure and optical properties of SnO₂

M. Maleki¹

Published online: 17 February 2020
© Springer Science+Business Media, LLC, part of Springer Nature 2020

Abstract

Nanostructured nitrogen-, niobium-, and tantalum-doped tin oxides are investigated by first-principle calculations. First, the band structure, bond length, density of states, and projected density of states of pure tin oxide are evaluated. Then, the effect of nitrogen, niobium, and tantalum doping substituting O and Sn is compared with the pure case. In all cases, substitutional doping with N results in *p*-type conductivity whereas *n*-type conductivity results from Nb and Ta doping. Substitution of O with N and of Sn with Nb or Ta increases the bandgap of the structure, while substitution of Sn and Nb with N reduces the bandgap.

Keywords Nitrogen · Niobium · Tantalum tin oxide · Siesta · DFT · Doping

1 Introduction

Transparent conducting oxides (TCOs) are defined as solid-state oxides that benefit from the properties of electrical conductivity and optical transparency at the same time [1]. SnO₂ is applied as a TCO material in different fields, namely gas sensors, solar cells, catalysis, etc. [2]. Pure SnO₂ is an intrinsic *n*-type material due to its native oxygen vacancy defects. Different elements have been studied as *p*- or *n*-type dopants using various simulation approaches [3–7]. Obtaining high transparency, low resistivity, and high mobility in TCOs—often contrasting requirements—requires compromises in the choice of the dopant that rely on the presence of oxygen vacancies. For an SnO₂-based TCO with *n*- or *p*-type conductivity, the appropriate dopant should supply more valence electrons or fewer conduction electrons than the Sn or O atoms and should have an ionic radius close or identical to that of Sn⁴⁺ or O²⁻. Based on the above statements, nitrogen may be a perfect choice as a *p*-type dopant due to its high solubility and nontoxicity. In addition, the ionic radius of N is close to that of the O atom. On the other hand, nitrogen as a group V atom has one fewer valence electron than O and one more valence electron than Sn, and thus is expected to

show amphoteric behavior in SnO₂. It may act as an acceptor when substituting on the O site but as a donor if incorporated at the Sn site [8]. It was therefore decided to investigate the effect of nitrogen doping at different substitutional sites. Nb and Ta are considered as acceptable selections for *n*-type TCO, since their ionic radii are close to those of the Sn atom [6]. However, they are substituted instead of oxygen atom to compare them with each other. On the other hand, the differences in the electronegativity and ionic radius between the host oxygen and the doping atom are effective factors for increasing or decreasing oxygen vacancies and modifying the electrical resistivity [9, 10].

Theoretical methods such as density functional theory (DFT) offer reliable approaches for predicting various properties of a large variety of semiconductors in an economic way [11]. In this study, the effect of tantalum, niobium, and nitrogen doping on tin oxide is investigated using DFT simulations in the Siesta code. The aim is to investigate the effect of doping at different positions of Sn site and O site in the lattice. Since *n*- and *p*-type materials play a key role in the preparation of different optoelectrical devices, it was decided to investigate the effect doping various materials using an economic simulation method.

✉ M. Maleki
m.maleki@fshiau.ac.ir

¹ Department of Physics, Faculty of Science, Fouman and Shaft Branch, Islamic Azad University, Fouman, Iran

2 Computational methods

The calculations are based on the fully self-consistent pseudopotential DFT method. Ab initio calculations in the local density approximation (LDA) are carried out according to the Ceperley–Alder (CA) parametrization along with the double-zeta basis set with polarization functions (DZP). Norm-conserving pseudopotentials as implemented in the SIESTA code [12] are used. A double-zeta basis function with polarization orbitals, a confining energy shift of 250 meV, and a mesh cutoff energy of 700 Ry for the grid integration are used. The Brillouin zone is sampled using a Monkhorst–Pack scheme with $(5 \times 5 \times 8)$ \mathbf{k} -point sampling. The optimized 48-atom SnO_2 supercell is constructed. To include substitutional defects, two models are introduced, viz. a doped atom substituting for a lattice Sn atom (X_{Sn}) and for an O atom (X_{O}), respectively. The doping percent of NSnO_2 (N_{O}), NSnO_2 (N_{Sn}), NbSnO_2 (Nb_{O}), NbSnO_2 (Nb_{Sn}), TaSnO_2 (Ta_{O}), and TaSnO_2 (Ta_{Sn}) is 0.58%, 0.61%, 3.87%, 4.05%, 7.5%, and 7.89%, respectively.

3 Results and discussion

3.1 Electronic structure

The band structure along the high-symmetry directions of the Brillouin zone of pure and N-doped SnO_2 in the two cases of substitution at O site and Sn site is evaluated and shown in Fig. 1. The bandgap in the pure case is about 2.1 eV at the highly symmetric Γ point, lower than the experimental value of 3.6 eV. It is well known that the bandgap is generally underestimated when using DFT [13]. The value of the bandgap is less than the experimental value since the LDA approximation for solids can decrease the bandgap in insulators and semiconductors due to the use of a potential which is the same for all the orbitals [14]. The valence-band maximum and the conduction-band minimum are located at the same Γ -point, indicating that the lowest bandgap transition in rutile SnO_2 is direct [11]. In the case of nitrogen substitution for tin, viz. NSnO_2 , narrowing of the bandgap due to insertion of new energy states into the gap is observed, which is a logical explanation for the red-shift of the photoluminescence observed in various studied [15–17], while in the case of N_{O} , the bandgap shows a minimal increase. Therefore, it can be concluded that this is due to the Burstein–Moss effect. From the curvature of the conduction band in nitrogen-doped tin oxide at the Γ -point [18], it can be concluded that the effective electron mass is less

than that of the hole while the effective electron mass in N_{O} (nitrogen instead of oxygen) is less than N_{Sn} (nitrogen instead of tin). So, the mobility of electrons in N_{O} is greater. The shift of the Fermi level toward the valence band shows that, in both cases of N_{O} and N_{Sn} , NSnO_2 is a p -type material.

In the cases of Nb and Ta doping, when Nb and Ta replace Sn, an increase in the bandgap is obvious, being due to the Burstein–Moss effect. However, when these two dopants substitute O, the bandgap shows a severe decrease. The large difference in ionic radii between Nb and Ta versus O causes the escape of oxygen atoms from the lattice [9]. Also, as the electronegativity difference between the two atoms in Nb–Sn and Ta–Sn bonds is not too great compared with the Sn–O bond, the oxygen deficiency increases [10]. The electronegativity of Nb, Sn, Ta, and O is 1.6, 1.8, 1.5, and 3.5, respectively. The curvature of the conduction band at the Γ -point reveals that the effective electron mass in Nb_{Sn} (Nb instead of tin) and Ta_{Sn} (Ta instead of tin) is less than Nb_{O} (Nb instead of oxygen) and Ta_{O} (Ta instead of oxygen). In addition, in all cases of Nb_{Sn} and Ta_{Sn} , the Fermi level enters the conduction band in the case of the Nb-doped SnO_2 and Ta-doped SnO_2 , resulting in degenerate n -type semiconductors; therefore, the Burstein–Moss effect can be predicted. This implies that the optical bandgap (from the top of the valence band to the Fermi level) expands significantly in the Nb- and Ta-doped SnO_2 system. Also, when Nb and Ta substitute for O, although the Fermi level enters the conduction band and these are n -type materials, the optical bandgap decreases due to the introduction of new levels in the gap as a result of the doping. The difference in the band structure between the two cases of Nb and Ta substitution at Sn site and O site can be related to the ionic radii of Nb and Ta compared with O and Sn.

The optimized 48-atom SnO_2 supercell is shown in Fig. 2a. For doping, we substituted one doped atom instead of one oxygen or tin atom. Six of the partial geometry structures are shown in Fig. 2b–g, respectively. In the structure of N_{Sn} , the optimal N–O bond length is 1.3717 Å and 1.3543 Å, revealing an inward relaxation compared with the Sn–O bond length of 2.0096 Å and 2.0828 Å (Fig. 2b). This occurs because the N atomic radius is smaller than the Sn atomic radius. In the case of N_{O} , the optimal bond length between the N atom and adjacent Sn atom is 2.0819 Å and 2.0746 Å, indicating a slight outward relaxation in comparison with the Sn–O bond length of 2.0828 Å and 2.0096 Å, respectively. This occurs because the N atomic radius is slightly larger than that of O (Fig. 1c) [13]. In the cases of the Nb_{Sn} models, the optimal bond length between the Nb atom and adjacent O atom is 2.0211 Å and 2.0283 Å, indicating a slight inward relaxation in comparison with the Sn–O bond length of 2.0828 Å and 2.0096 Å. This occurs because the Nb atomic radius is slightly smaller than that

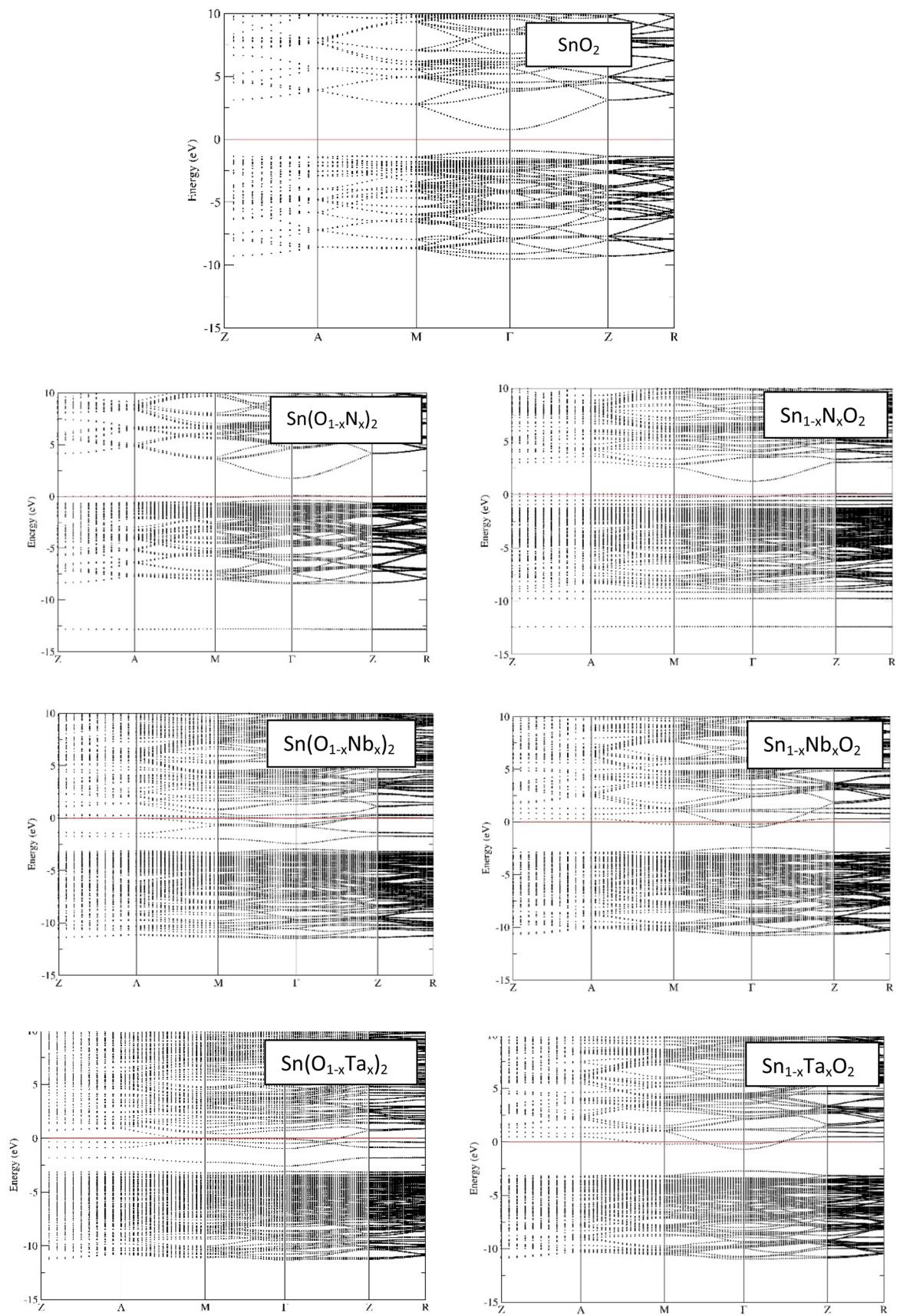


Fig. 1 The band structure of pure and doped tin oxide

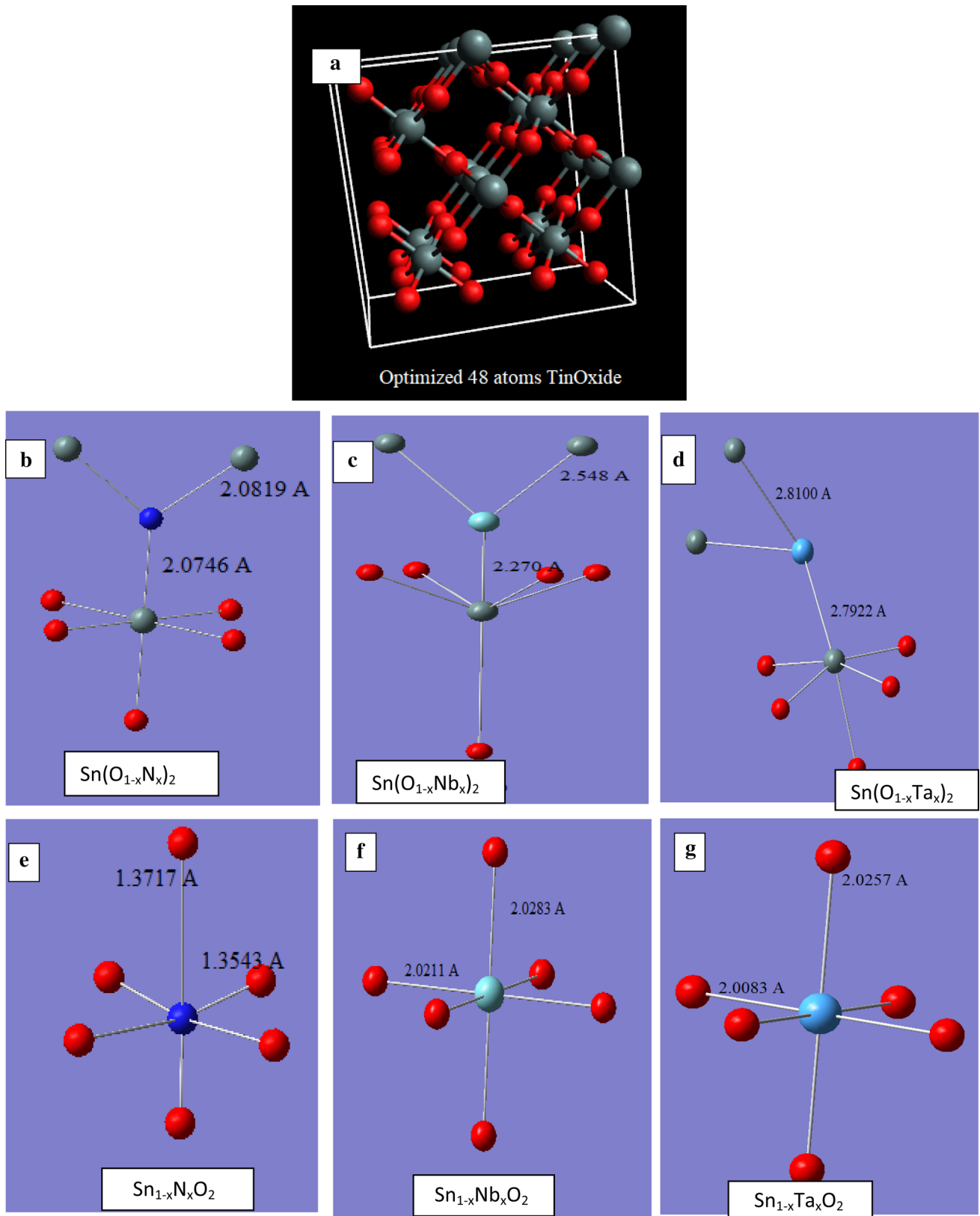


Fig. 2 The supercell and partial geometry of pure and doped tin oxide: **a** 48-atom tin oxide, **b** N_{Sn} , **c** N_O , **d** Nb_{Sn} , **e** Nb_O , **f** Ta_{Sn} , and **g** Ta_O (red balls are O, gray balls are Sn, and blue balls are N, Ta, or Nb) (Color figure online)

of Sn (Fig. 1d). In the cases of the Nb_O models, the optimal bond length between the Nb atom and adjacent Sn atom is 2.5482 Å and 2.2704 Å, indicating a slight outward relaxation in comparison with the Sn–O bond length of 2.0828 Å and 2.0096 Å. This occurs because the Nb atomic radius is larger than that of O (Fig. 1e). In the cases of the Ta_Sn models, the optimal bond length between the Ta atom and adjacent O atom is 2.0083 Å and 2.0257 Å, indicating an inward relaxation in comparison with the Sn–O bond length of 2.0828 Å and 2.0096 Å. These results are comparable to Darriba's investigations on Ta:SnO₂ [18]. This occurs because the Ta atomic radius is slightly smaller than that of Sn (Fig. 1f). In the cases of the Nb_O models, the optimal bond length between the Nb atom and adjacent Sn atom is 2.8100 Å and 2.7922 Å, indicating outward relaxation in comparison with the Sn–O bond length of 2.0828 Å and 2.0096 Å. This occurs because the Nb atomic radius is bigger than that of O (Fig. 1g). Also, in all the above cases of doping, adjacent atoms near the defective region have a tendency to be displaced to find new equilibrium positions.

The discussion above illustrates that a dopant atom bigger than O tends to disturb the whole structure of the unit cell, while substitution for Sn does not disrupt the structure.

The density of states (DOS) and projected density of states (PDOS) of pure tin oxide are depicted in Fig. 3.

Figure 3 shows the three main peaks of undoped SnO₂ at about -7, -4, and -1 eV. The peak at -7 eV is a bonding orbital originating from interactions between Sn 5s and a symmetrical combination of the six O 2p orbitals; the peak at -4 eV is a result of the *ppσ* bonding orbital containing Sn 5p, p, and O 2p orbitals, whereas the peak at -1 eV is because of the nonbonding O 2p orbital. Also, the lower part of the conduction band is made up of a peak at 5 eV due to the antibonding Sn 5s–O 2p orbital, and some peaks between 7 and 12 eV are due to the antibonding Sn 5s–O

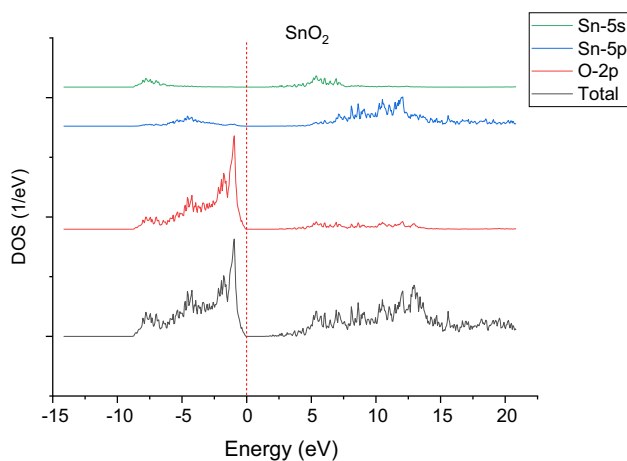


Fig. 3 The DOS and PDOS of pure tin oxide

2p orbital. The features of the DOS of undoped SnO₂ are in good agreement with other calculations [19].

Figures 4 and 5 show the projected density of states (PDOS) of N-doped SnO₂. N doping does not change the total DOS of the SnO₂ unit cell, except for the position of the Fermi level.

As mentioned above, the upper contribution of the valence band, for undoped SnO₂, mainly corresponds to the O 2p states with a slight contribution from Sn 5p states. The bottom part of the conduction band basically derives from Sn 5p and Sn 5s states, while O 2p states also make a small contribution. Mainly, the N 2p states start to mix with the valence-band edge of SnO₂ in both cases of N_O and N_Sn sites. In N-doped SnO₂, the major effects on the band structure are to form acceptor states and move the Fermi level toward the valence-band maximum, resulting in *p*-type conducting semiconductors. In addition, the Fermi level enters the valence band in both cases of N-doped SnO₂ with N_O and

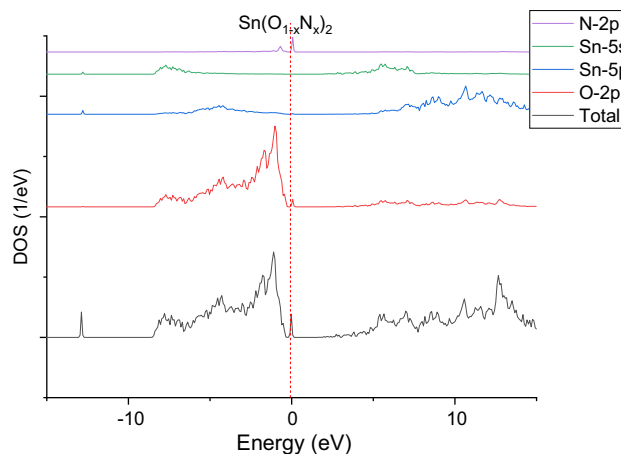


Fig. 4 The DOS and PDOS of NSnO₂ (N instead of O)

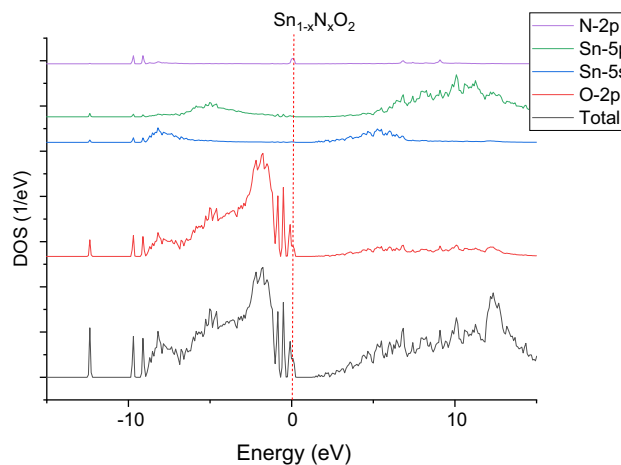


Fig. 5 The DOS and PDOS of NSnO₂ (N instead of Sn)

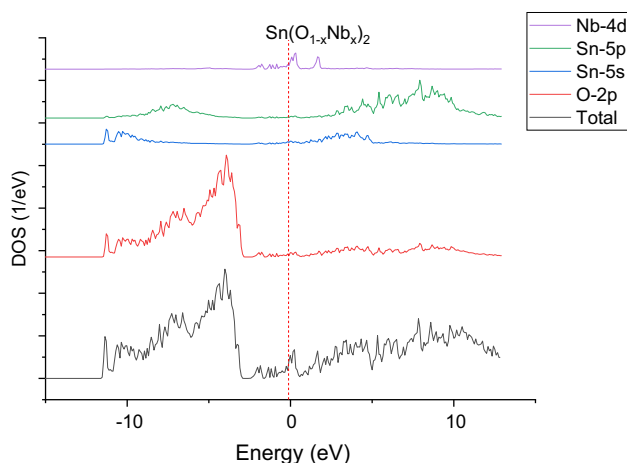


Fig. 6 The DOS and PDOS of Nb-doped SnO_2 (Nb instead of O)

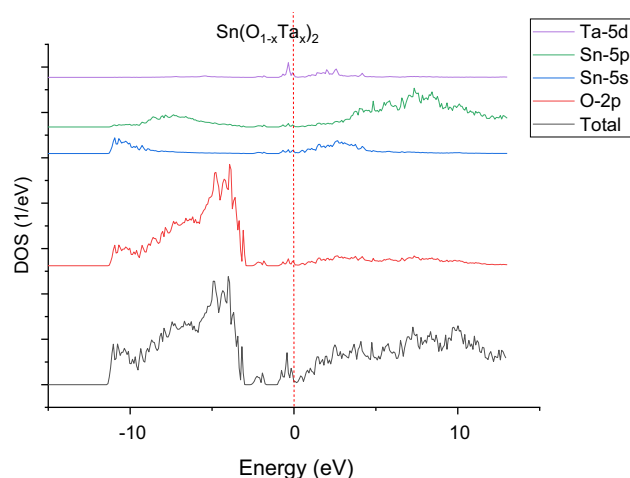


Fig. 8 The DOS and PDOS of Ta-doped SnO_2 (Ta instead of O)

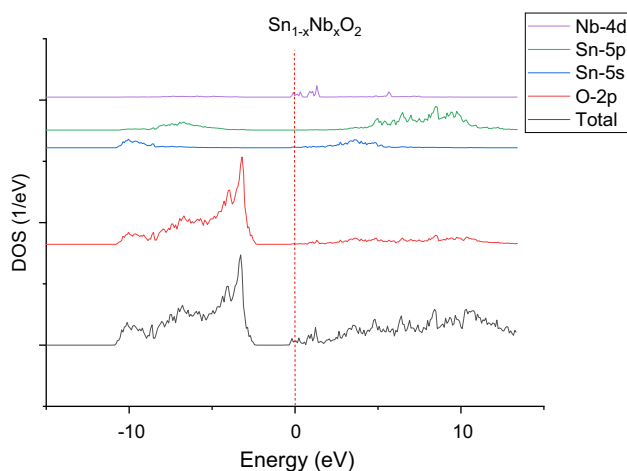


Fig. 7 The DOS and PDOS of Nb-doped SnO_2 (Nb instead of Sn)

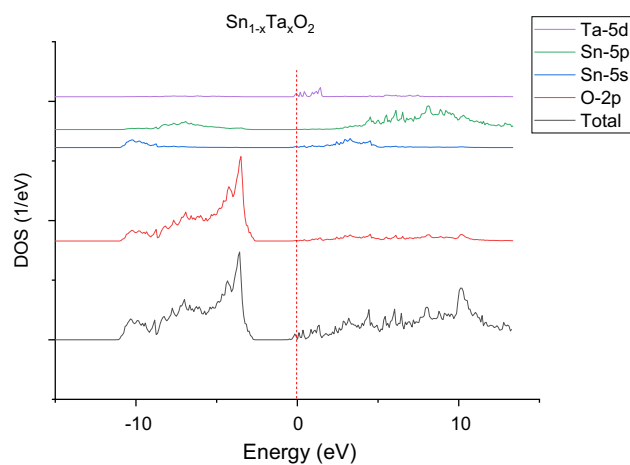


Fig. 9 The DOS and PDOS of Ta-doped SnO_2 (Ta instead of Sn)

N_{Sn} substitution [13–15]. These results are in good accordance with those of Sun et al. [20].

The density of states and projected density of states of Nb-doped tin oxide and Ta-doped tin oxide substituted instead of O and N depicted in Figs. 6, 7, 8 and 9 show that Nb_{Sn} , Nb_{O} , Ta_{Sn} and Ta_{O} show n-type character, which are in accordance with the theoretical publications by Slassi et al. [11] and Qin et al. [21].

In the cases of the Nb_{O} and Ta_{O} substitutions, the Nb 4d and Ta 5d states start to mix with the conduction-band edge of SnO_2 , leading to an obvious splitting above E_{F} and thus resulting in obvious bandgap narrowing in the Nb- and Ta-doped supercell. In Nb- and Ta-doped SnO_2 , the major effects on the band structure are to form donor states and move the Fermi level toward the conduction-band minimum, resulting in an n-type conducting semiconductor. In addition, the Fermi level enters the conduction band in all cases

of Nb- and Ta-doped SnO_2 substitution at O and Sn sites. In the cases of Nb_{Sn} and Ta_{Sn} sites, the bandgap increases due to the Burstein–Moss effect. The results for Nb-doped tin oxide (Fig. 6) show that the introduction of Nb impurities causes degeneracy of the Nb-doped SnO_2 , as the Nb atoms act as donor-type impurities. The lower part of the conduction band formed by a peak at about -2 eV is due to Sn 5s, Sn 5p, O 2p, and Nb 4d orbitals. These combined orbitals indicate bonding interactions among Sn, O, and Nb atoms. Figure 7 shows the DOS and PDOS of Nb-doped SnO_2 substituting Nb instead of Sn. The introduction of these impurities causes the Fermi level to enter the conduction band. This result indicates degeneracy of Nb-doped SnO_2 . The lower part of the conduction band formed by a peak at -4 eV is due to Sn 5s, Sn 5p, O 2p, and Nb 4d orbitals. From these results, it is clear that Nb atoms act as donor-type impurities. On the other hand, Fig. 8 indicates that the Ta 5d orbitals are

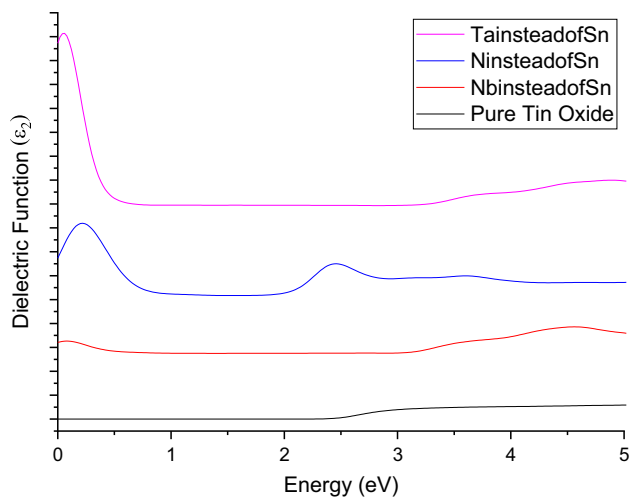


Fig. 10 The imaginary part of the dielectric function of pure and N-, Nb-, and Ta-doped SnO₂ with substitution for Sn

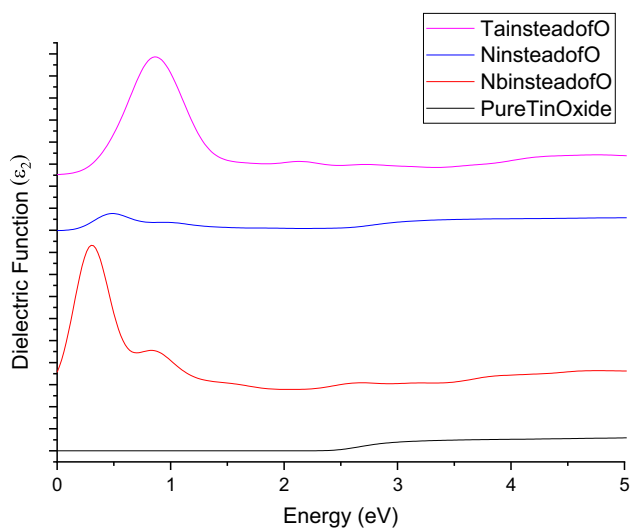


Fig. 11 The imaginary part of the dielectric function of pure and N-, Nb-, and Ta-doped SnO₂ with substitution for O

found within the valence and conduction bands. The lower part of the conduction band is formed by a peak at -2 eV, which is due to Sn $5s$, Sn $5p$, O $2p$, and Ta $5d$ orbitals. These results indicate degeneracy of Ta-doped SnO₂ because the Ta atoms act as donor-type impurities. The same results are seen for Ta-doped SnO₂ (Ta instead of Sn) at an energy of about -4 eV.

3.2 Optical properties

The imaginary part of the dielectric function of pure and N-, Nb-, and Ta-doped SnO₂, substituting for Sn and O, is shown in Figs. 10 and 11, respectively.

The optical calculations are carried out using a $5 \times 5 \times 8$ optical mesh and optical broadening of 0.05 eV [22].

The transition energy threshold related to the energy peak at about 2.6 eV corresponds to the bandgap of pure SnO₂, which is in accordance with the work of Slassi [11]. This threshold moves to a lower energy of about 2.2 eV and 2.1 eV in the case of the Nb_O- and Ta_O-doped SnO₂ systems, respectively. This red-shift can be explained by the decreased bandgap due to such doping. The peak at energy of 2.7 eV in the case of N_O-doped SnO₂ shows a small blue-shift due to the nitrogen doping, indicating acceptable changes in the optical transparency due to such doping of TCO materials. In the case of substitution of the doping atom for Sn, a blue-shift is seen in the case of Nb- and Ta-doped SnO₂ due to the Burstein–Moss effect. The peak at 3.3 eV is related to Nb-doped SnO₂, whereas the peak at 3.4 eV is related to Ta-doped SnO₂, while the peak at 2.1 eV is related to N-doped SnO₂. In the case of N doping for Sn, a decrease in the bandgap is observed. Moreover, the peaks at energies of about 0.2 and 0.5 eV correspond to the electron transition between occupied and unoccupied states localized just around the Fermi level. These low energies of the electron transition suggest that electron injection into the conduction band could start from a low excitation energy in the Nb- and Ta-doped SnO₂ samples, which is useful for transparent electrode applications.

4 Conclusions

The effect of nitrogen, niobium, and tantalum doping for Sn and O atoms at different positions in tin oxide is studied by using the fully self-consistent pseudopotential DFT method. In comparison with undoped tin oxide, the bandgap of doped tin oxide reduces in the cases of N_{Sn}, Nb_O, and Ta_O but increases in the cases of N_O, Nb_{Sn}, and Ta_{Sn}. Also, depending on the atomic radius of the dopant, the bond length increases or decreases in comparison with the pure case. The DOS and PDOS reveal that substitution of N instead of either Sn or O leads to *p*-type conductivity, while substitution of either Nb or Ta for O or Sn causes *n*-type conductivity. The optical properties are found to be in accordance with the band structures.

Acknowledgements This project was supported by the Islamic Azad University, Fouman and Shaft Branch, Iran. The author appreciates the friendly help of Dr. Sepahi with this project.

References

- Godinho, K.G., Walsh, A., Watson, G.W.: Energetic and electronic structure analysis of intrinsic defects in SnO₂. *J. Phys. Chem. C* **113**, 439–448 (2009)

2. Valentin, D., Nature, E., Albanese, E., Di Valentin, C., Pacchioni, G., Sauvage, F.: Nature of paramagnetic species in nitrogen-doped SnO₂. *J. Phys. Chem. C* **119**(48), 26895–26903 (2015)
3. Ziat, Y., Slassi, A., Zarhri, Z., Hammi, M., Houmad, M., Ait Raiss, A., Sbai, Y., Echih, S., El Kenz, A., Benyoussef, A.: First-principles study of magnetic and electronic properties of fluorine-doped Sn_{0.98}Mn_{0.02}O₂ system. *J. Supercond. Nov. Magn.* **29**, 2979–2985 (2016)
4. Wang, T., Zhang, H., Tian, L., Li, Y., Zhang, Y., Cui, S., Ding, Y., Tang, J., Zhang, R.: Electronic structure and optical properties of oxygen vacancy and Ag-doped SnO₂ sensors. *Chem. Eng. Trans.* **51**, 1285–1290 (2016)
5. Mudarra Navarro, A.M., Rodríguez Torres, C.E., Cabrera, A.F., Weissmann, M., Nomura, K., Errico, L.A.: Ab initio study of the ferromagnetic response, local structure, and hyperfine properties of Fe-doped SnO₂. *J. Phys. Chem. C* **119**(10), 5596–5603 (2015)
6. Zhang, G., Qin, G., Yu, G., Hu, Q., Fu, H., Shao, C.: Ab initio investigation on a promising transparent conductive oxide, Nb:SnO₂. *Thin Solid Films* **520**, 5965–5970 (2012)
7. Fakhim Lamrani, A., Belaiche, M., Benyoussef, A., Kenz, E.: Electronic structures and ferromagnetism of SnO₂ (rutile) doped with double-impurities: first-principles calculations. *J. Appl. Phys.* **115**, 013910 (2014)
8. Varley, J.B., Janotti, A., Van de Walle, C.G.: Group-V impurities in SnO₂ from first-principles calculations. *Phys. Rev. B* **81**, 245216 (2010)
9. Patil, S., Seal, S., Guo, Y., Schulte, A., Norwood, J.: Role of trivalent La and Nd dopants in lattice distortion and oxygen vacancy generation in cerium oxide nanoparticles. *Appl. Phys. Lett.* **88**, 24110 (2006)
10. Kim, C.H., Rim, Y.S., Kim, D.L., Kim, H.J.: Combined effect of the large ionic radius and low electronegativity of lanthanum additive on solution-processed zinc–tin–oxide thin-film transistors. *Thin Solid Films* **536**, 291 (2013)
11. Slassi, A.: Ab initio study on the structural, electronic, optical and electrical properties of Mo-, Nb- and Ta-doped rutile SnO₂. *Opt. Quantum Electron.* **48**, 160 (2016)
12. Soler, J.M., Artacho, E., Gale, J.D., Garcia, A., Junquera, J., Ordejon, P., Sanchez-Portal, D., García, A., Junquera, J., Ordejón, P., Sánchez-Portal, D.: The SIESTA method for ab initio order-N materials simulation. *J. Phys. Condens. Matter.* **14**, 2745 (2002)
13. Mazzone, A.M., Morandi, V.: CO adsorption onto tin oxide clusters: DFT calculations. *Comput. Mater. Sci.* **38**, 814–823 (2007)
14. Ziat, Y., Hammi, M., Zarhri, Z., Laghlmi, C., Rhazouani, O.E.: Ferrimagnetism and ferromagnetism behavior in (C, Mn) co-doped SnO₂ for microwave and spintronic: Ab initio investigation. *J. Magn. Magn. Mater.* **483**, 219–223 (2019)
15. Xing, C.W., Wang, D.X., Zhang, P.J.: The electronic structures and optical properties in nitrogen-doped SnO₂. In: 4th Annual International Conference on Material Science and Engineering (ICMSE 2016), 2016
16. Long, R., English, N.: Density functional theory description of the mechanism of ferromagnetism in nitrogen-doped SnO₂. *Phys. Lett. A.* **374**(2), 319–322 (2009)
17. Guipeng, S., Jinliang, Y., Peijiang, N., Delan, M.: Electronic structure and optical property of p-type Zn-doped SnO₂ with Sn vacancy. *J. Semicond.* **37**(2), 023005 (2016)
18. Darriba, G.N., Muñoz, E.L., Errico, L.A., Rentería, M.: Ab initio study of structural, electronic, and hyperfine properties of n-type SnO₂: Ta semiconductor. *J. Phys. Chem. C* **118**, 19929–19939 (2014)
19. Oshima, M., Yoshino, K.: Structural and Electronic Structure of SnO₂ by the First-Principle Study, vol. 725, pp. 265–268. Trans Tech, Stäfa (2012)
20. Sun, X., Long, R., Cheng, X., Zhao, X., Dai, Y., Huang, B.: Structural, electronic, and optical properties of N-doped SnO₂. *J. Phys. Chem. C* **112**(26), 9861–9864 (2008)
21. Qin, G., Zhang, G., Liu, S., Fu, H., Wen, J.: Ab initio study on Ta:SnO₂. *Adv. Mater. Res.* **160**, 574–578 (2011)
22. Nabi, Z., Kellou, A., Mecabih, S., Khalfi, A., Benosman, N.: Opto-electronic properties of rutile SnO₂ and orthorhombic SnS and SnSe compounds. *Mater. Sci. Eng. B* **98**, 104–115 (2003)

Publisher's Note Springer Nature remains neutral with regard to jurisdictional claims in published maps and institutional affiliations.